Nature Environment and Pollution Technology
An International Quarterly Scientific Journal

p-ISSN: 0972-6268
(Print copies up to 2016)
e-ISSN: 2395-3454

Vol. 22 | No. 4 | pp. 2129-2136 | 2023

Original Research Paper

https://doi.org/10.46488/NEPT.2023.v22i04.038

Open Access Journal

Effect of Fulvic Acid on the Denitrification in Deep Subsurface Wastewater Infiltration System

Jingjing Lv*, Jingjing Li, Yanyan Dou*, Guoke Chen*, Yubing Ye*** and Li'an Hou****†**

*College of Energy and Environmental Engineering, Zhongyuan University of Technology, Zhengzhou 450007, China
**CSCEC Zhongyuan Architectural Design Institute Co. Ltd., Zhengzhou 450004, China
***Shanghai Municipal Engineering Design Institute Co. Ltd., Shanghai 200092, China
****College of Environmental Science and Engineering, Tongji University, Shanghai 200092, China
†Corresponding author: Li'an Hou; houla@cae.cn

Nat. Env. & Poll. Tech.
Website: www.neptjournal.com

Received: 12-04-2023
Revised: 31-05-2023
Accepted: 06-06-2023

Key Words:
Denitrification
Organic composition
Wastewater infiltration system
Fluorescence analysis

ABSTRACT

This work aims to explore the impact of fulvic acid (FA) on denitrification within the purification process of sewage in the deep subsurface wastewater infiltration system (DSWIS). In the system, an organic glass column (height = 2.40 m; radius = 0.30 m) was filled with several layers of soil. Simulated domestic wastewater and extracted FA from landfill leachate were used in the experiments. It was found that before and after the addition of FA, COD, and NH_4^+-N were efficiently removed when a hydraulic load was 8 $cm \cdot d^{-1}$. Moreover, after FA addition, the removal efficiency of TN was enhanced from 67.74% to 78.01%. Organic matter transformation analysis indicated that in the under part, the shortage of carbon sources limited the denitrification prior to FA addition, resulting in a low TN removal efficiency. However, after adding FA, more FA-like substances were transferred into protein-like matters than before the addition of FA, which has helped produce more easily biodegradable organics for denitrification. So, the addition of FA could enhance the denitrification process in the system of DSWIS.

INTRODUCTION

It has been proved that a soil wastewater infiltration system (SWIS) could be an efficient and cost-on-site alternative advanced strategy to deal with wastewater (Chen et al. 2021, Lv et al. 2019, Zheng et al. 2018a, Yang et al. 2020). Nowadays, SWIS has been largely implemented to treat wastewater in various countries, like China, Japan, and the United States (Lv et al. 2020, Yuan et al. 2016, Xu et al. 2020, Eregno & Heistad 2019, Kawasaki 2019.). In SWIS, traditional biological or physical-chemical approaches are firstly applied to treat wastewater; afterward, the treated wastewater is penetrated through an aerated unsaturated zone; during the penetration, wastewater is purified via a series of processes, including adsorption, chemical reaction, filtration, and biodegradation. Compared to the traditional process of the activated sludge, SWIS exhibits various advantages, covering easy operation and maintenance, low cost of manufacture and execution, and excellent performance in removing total phosphorus (TP) and chemical oxygen demand (COD) (Li et al. 2021a, Yamaguchi et al. 1996). In addition, more than 80% removal efficiencies were achieved for TP, suspended solids, and organic compounds (Payne et al. 2017, Christianson et al. 2017, Yang et al. 2021, Bieber et al. 2018).

However, it was previously reported by many studies that SWIS was not sufficient to remove nitrogen. Depending on the operation conditions, wastewater composition, and environmental conditions, 10-90% removal efficiency of total nitrogen (TN) could be yielded (Gu et al. 2019, Jia et al. 2023, Qin et al. 2021, Li et al. 2021b, Yang et al. 2022, Li et al. 2023).

Additionally, it has been indicated that in the subsurface infiltration systems, denitrification and nitrification serve as the two primary reactions involved in eliminating nitrogen from sewage water, while other processes, including ammonia volatilization, grass uptake, and substrate adsorption, are generally of less significance (Li et al. 2021a, Perujo et al. 2017, Yu et al. 2019). However, during the percolation process, denitrification and nitrification can occur in the same unit of soil infiltration. Nitrification and decomposition of organic substrates typically appear in the upper area containing enough oxygen. However, denitrification primarily occurs in the lower area where organic matter barely remains and oxygen is strictly absent.

Therefore, in the lower part, the shortage of carbon sources greatly contributes to the low elimination of TN and low denitrification (Jia et al. 2019, Shokri et al. 2021, Su et al. 2023).

Different research has been conducted to solve this problem. Zheng et al. (2018b) demonstrated that shunt-distributing wastewater promoted decreased oxygen concentration in the system, establishing a good environmental condition for denitrification. According to the study of Nakhla and Farooq (2003), it was found that in the slow sand filters, slowly biodegradable COD and particulate could be used for denitrification. Ye et al. (2008) designed a system of a two-stage anaerobic tank integrated with a soil trench. In the system, 60% and 40% of the raw sewage was individually transferred into the first and second anaerobic tanks. In the soil trench, 40% of raw sewage provided the necessary carbon source, leading to a high nitrogen removal rate.

Moreover, various research has demonstrated that successful denitrification was associated with the depth of the SWIS. It has been proved that in a DSWIS, the optimal depths for the reactions of denitrification and nitration were 0.70-1.50 m and 0.30-0.70 m, individually (Li et al. 2021). However, for the traditional SWISs, the optimal depths were < 1.2 m (varying between 0.6 and 1.2 m), where the process of denitrification was prevented due to the presence of an anaerobic environment (Ye et al. 2008). It was also revealed that the optimal depth to remove the total nitrogen (TN) in SWIS was 1.55 m, where TN was effectively eliminated (Li et al. 2021). Zhang et al. (2015) also achieved good performance of nitrogen removal in the soil column with a 2.00 m depth, and 83.68 and 99.77% removal efficiencies were obtained for TN and NH_4^+-N. Furthermore, it has been observed that the refractory organics, fulvic acid-like (FA-like) substances, were partly degraded at 1.05-1.30m and transferred into protein-like substances, which led to a leap of TN elimination. It might indicate that the FA-like substances were able to serve as carbon sources for denitrification.

Hence, we checked if FA could be used as the biodegradable carbon source to facilitate removing nitrogen in DSWIS. Furthermore, we investigated the impact of FA on nitrogen removal efficiency. A soil column with a depth of 2.00 m was utilized to simulate a subsurface soil infiltration system. Nitrogen and organic matter variations in the whole percolation process will be studied. Then, the nitrogen and organics removal performances before and after the addition of FA would be compared. Moreover, the exact effect mechanisms of FA on denitrification will be analyzed.

MATERIALS AND METHODS

Description of the Pilot System

The material of the pilot system column is organic glass. The height and radius of the column are 2.40 m and 0.30 m. It is composed of four segments connected using flanges. From the top to the bottom, the lengths of segments are 0.50, 0.50, 0.70, and 0.70 m, respectively. Before securing each segment together, a gasket is located between the two segments to keep a watertight seal. Three parallel experiments were conducted. Fig.1 displays the schematic of the soil column.

Materials

In this study, the soil was obtained from the Shunyi District of Beijing. To simulate the real soil condition, the soil depth in the organic glass column was the same as in the original soil location. From top to bottom, the soil densities in the column were 1.43, 1.56, 1.63, and 1.76 g·cm^{-3} at 0~0.50,

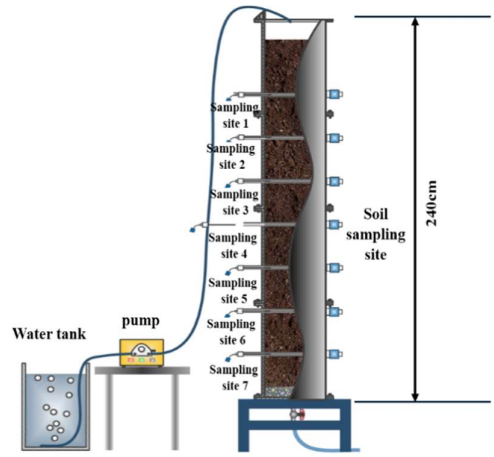

Fig. 1: Setup of the soil column. There are seven sampling sites. They are set at 0.20, 0.50, 0.80, 1.10, 1.40, 1.70, and 2.00 m, where water samples would be obtained using in-situ soil solution samplers.

Table 1: The exacted components from the sewage.

Drag names	Concentration ($mg \cdot L^{-1}$)
Sucrose	200.0
Peptone	220.0
ammonium chloride	117.0
ferric chloride	0.4
magnesium sulfate heptahydrate	62.0
dipotassium phosphate	44.0
boric acid	10.0
copper sulfate pentahydrate	0.8
potassium iodide	1.9
manganese sulfate dihydrate	7.8
sodium molybdate dihydrate	4.0
zinc sulfate heptahydrate	7.8
calcium chloride dihydrate	1.9
sodium nitrate	91.0

0.50~1.00, 1.00~1.50, and 1.50~2.00 m. Once filled with soil, the column was thoroughly covered by black plastic tarps to avoid the growth of algae and the effect of light during operation.

The sewage in the experiment was used to simulate domestic wastewater. The components extracted from the sewage are listed in Table 1. A silicone tube transferred wastewater into the column using a variable-speed peristaltic pump.

The FA used in the experiment was extracted from landfill leachate of A Su Wei landfill field in Beijing, China. XAD-8 and hydrogen-type cation exchange resin were used to isolate and purify the FA (Stevenson & Cole 1999). Then, the purified FA solution was dehydrated by a freezer dryer, and the FA powder was preserved in valve bags.

After the column was set up, tap water was transferred to the soil column to eliminate the original pollutants in the soil for 3 months. Afterward, the 24-hour composite percolate was analyzed for sequential three days. The results indicated that there are no constituents leached ($TP < 0.01\ mg \cdot L^{-1}$, $TN < 1\ mg \cdot L^{-1}$, and $COD < 10\ mg \cdot L^{-1}$). Subsequently, simulated wastewater was delivered into the soil column for three months for the start-up and domestication of the system. At last, a hydraulic load was set as $8\ cm \cdot d^{-1}$ and the detailed experiments were performed in the continuous feeding mode for one year.

Test of Soil Adsorption

Batch adsorption tests were carried out to evaluate the adsorption capacities of NH_4^+-N by the soils. A constant weight of soil samples was obtained by drying at 105°C. Prior to sterilization for 30 min at 121°C and 1.1 MPa, 5 g of dried soil sample was taken out from different depths (0-0.50, 0.50-1.00, 1.00-1.50 and 1.50-2.00 m) and transferred in 250 mL conical flasks. Certain volumes of solution containing various levels of NH_4^+-N were placed into each flask. The samples in the flasks were agitated at the seed of 160 rpm for 24 h at 25°C. When equilibrium was observed in adsorption, the solution was filtered through a membrane (0.45 μm). According to Zhang et al. (2020), the following formula could be employed to compute the adsorption capacity of NH4+-N by the soil:

$$q = (C_0\text{-}C)V/M \quad \ldots (1)$$

Where q represents the soil adsorption capacity, $mg \cdot g^{-1}$; M represents the soil dry weight, g; C_0 and C individually represent the initial and equilibrium levels of the target component in the solution of mixed soil, $mg \cdot L^{-1}$; and V represents the solution volume, L.

Sample and Data Analysis

After the soil system ran stably, samples at the influent, effluent, and seven sampling points of the system were collected weekly. A dichromate approach was employed to determine the concentration of COD. The Multin N/C 2100 TOC/TN tester was implemented for the quantification of the total organic carbon (TOC). Standard approaches according to E.P.A. (2002) were applied to measure the levels of TN, nitrate nitrogen (NO_3^--N), nitrite nitrogen (NO_2^--N), and ammonia nitrogen (NH_4^+-N). All samples were tested on the same day when they were sampled. The organic composition and stabilization of samples were evaluated by using fluorescence spectroscopy.

Each sample was conducted at ambient temperature (~25°C) by 3D excitation-emission matrix (3D-EEM) fluorescence spectroscopy using a luminescence spectrophotometer (F-7000 FL spectrophotometer, Hitachi, Japan). Samples were continuously scanned with the speed of 2400 nm·min-1 at 5 nm intervals. The emission and excitation wavelengths were 260 to 550 nm and 200 to 450 nm, individually (Elliotts et al. 2006, Chen et al. 2003). The width of the slit was 10 nm for emission and excitation monochromators. Before the fluorescent measurement, the samples would be diluted below $10\ mg \cdot L^{-1}$.

3D-EEM integrated with parallel factor (PARAFAC) analysis was comprehensively used to evaluate the change of dissolved organic matter (DOM), which could help to obtain the DOM variation regularity (Urban-Rich et al. 2006). Over the past two decades, it has been widely reported that PARAFAC could be successfully utilized to decompose EEMs of complex mixtures into their individual fluorescent components (Mazivila et al. 2020, Zhang et al. 2020). The

Table 2: This was Langmuir's model of adsorption isotherms of ammonia nitrogen.

Model	Soil depth (cm)	Fitted equations	y, x	Correlation coefficient (R^2)
Langmuir	0-50	y=3.24x+149.6	y=Ce/qe	0.94
	50-100	y=3.06x+97.2	x=Ce	0.99
	100-150	y=2.19x+101.7	Ce: Equilibrium concentration	0.98
	150-200	y=3.17+187.4	Qe: Equilibrated adsorption capacity	0.95

PARAFAC model of EEMs was elucidated by Markager et al. (2011). Before PARAFAC modeling, FL solution 4.0 and DOM Flour toolbox (MATLAB 2009a) were used to wipe off the influence of Raman and Rayleigh scattering.

RESULTS AND DISCUSSION

Ammonia Nitrogen Adsorption Process

The observed data were fitted to the Langmuir isothermal adsorption model based on the study reported by Zhang et al. (2015).

The saturated adsorption capacities of the soils in various depths were 0.32, 0.37, 0.34, and 0.26 $mg \cdot g^{-1}$ from the top to the bottom (Table 2). Considering the densities of different layers, the total adsorption capacities were 16.16, 20.38, 19.57, and 16.16 g, respectively.

The ammonia nitrogen removal efficiencies were above 98% during all the experiments at 1.10 m depth. Therefore, the soil at 0~1.10 m played the most important role in ammonia nitrogen elimination. Moreover, the maximal ammonia nitrogen adsorption capacity at 0~1.50 m was 16.16 + 20.38 + 19.57 = 56.11 g. Since the average level of ammonia nitrogen flowed in was 35.33 $mg \cdot L^{-1}$, the load of influent ammonia nitrogen was 35.33 × 0.08 × 3.14 × 0.32 = 0.8$g \cdot d^{-1}$, and the maximal saturation adsorption time was 56.11/0.8 = 70.14 d. Nevertheless, the start-up and domestication time of the system was three months (90 d), and the operation time lasted one year. Therefore, the soil adsorption exhibited no impact on the removal of nitrogen.

Performances Before and After the Addition of FA

As shown in Fig. 2, trends in COD changes before and after the addition of FA were similar, and the organic matter degradation process could be divided into three parts. In part, at the depth of 0~0.20 m, 40.72% and 39.29% of COD were rapidly degraded before and after adding FA, which mainly contributed to the aerobic decomposition process of organic matter. Certainly, the nitrifying process of ammonia nitrogen, which was restricted because of the high concentration of oxygen and organic matter, and other possibly existing processes consumed a small amount of organic matter. In part II, at a depth of 0.20~1.10 m, due to the gradually decreasing dissolved oxygen concentration, the removal rate of COD

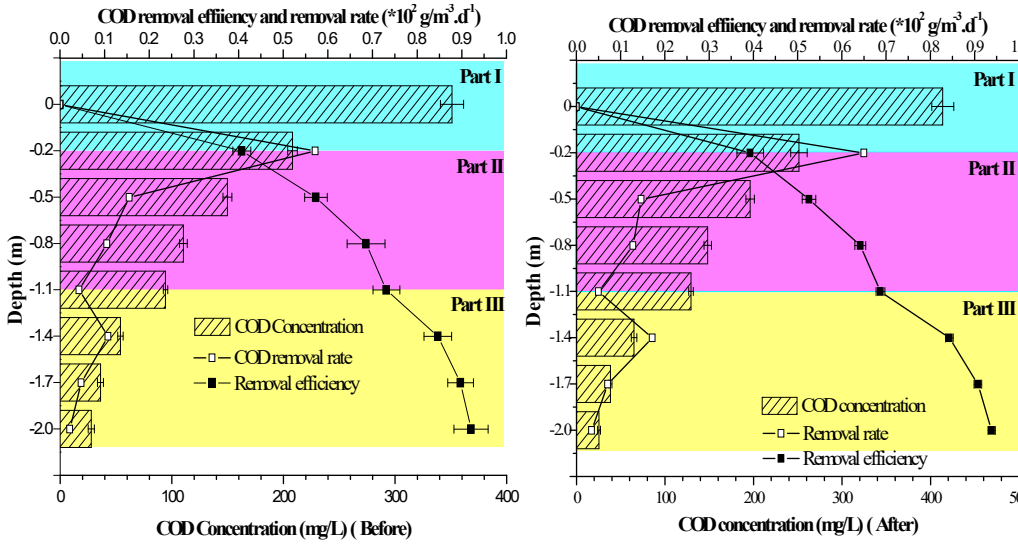

Fig. 2: Variation of COD along the depth before and after the addition of FA. Variation of COD concentration, COD removal efficiency, and removal rate before the addition of FA (left); Variation of COD concentration, COD removal efficiency, and removal rate after the addition of FA. In the figures, error bars were the values of standard deviations (right).

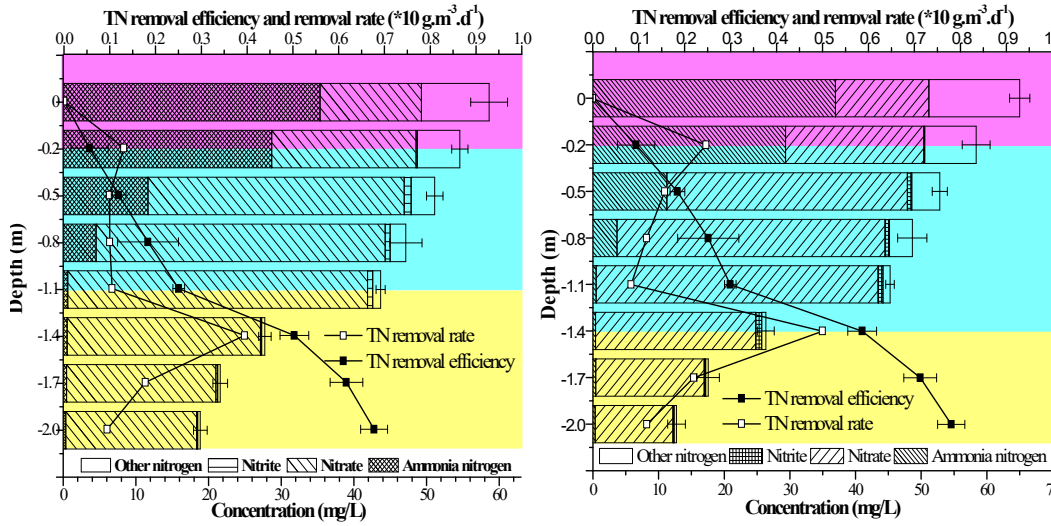

Fig. 3: Variation of TN, NO_2^--N, NO_3^--N, and NH_4^+-N along with the depth of soil column. Variation of TN, NO_2^--N, NO_3^--N, NH_4^+-N concentration, removal efficiency, and removal rate before the addition of FA (left); Variation of TN, NO_2^--N, NO_3^--N, NH_4^+-N concentration, removal efficiency, and removal rate after the addition of FA. In the figures, error bars were the values of standard deviations (right).

was reduced gradually. In part III, the COD removal rate experienced a rise and then fell. Especially at 1.10~1.40 m, the COD removal rate had a shape rise, which meant some reactions that consumed a great amount of organic matter occurred.

In general, the addition of FA promoted the nitrogen removal process. TN removal efficiency increased to 78.01% after the addition of FA from 67.74%. The nitrogen removal amount was also improved from 39.70 to 50.95 $mg \cdot L^{-1}$.

Nitrification and denitrification were reported to be mainly related to the removal of TN. The nitrification mainly occurred in parts I and II, where more than 98% of ammonia nitrogen was eliminated, so the shape rises of the COD removal rate in part III had little relation with ammonia nitrogen variation. Meanwhile, as shown in Fig. 3, nitrate nitrogen accounted for more than 93% of TN in part III, and the elimination of TN was mainly due to the degradation of nitrate nitrogen, which demonstrated the occurrence of denitrification. That was to say. It was the denitrification process that caused the COD variation in part III.

In part I, before the addition of FA, the nitrification process was seriously limited at 0~0.20 m. The reason might be attributed to the shortage of carbon sources. As described above, nitrification was greatly restricted because of the high concentration of oxygen and organic matter in part I. As organic nitrogen was decomposed and another possible denitrification process was presented, only a small amount of TN was eliminated. Nevertheless, in part II, the nitrification rate reached the maximum at 0.20~0.50 m and then gradually decreased because of the gradually decreasing concentration of dissolved oxygen and the existence of organic matter. The ammonia nitrogen removal efficiency reached 98.25% at 1.10 m, and only 25.06% of TN was eliminated at 0~1.10 m. In part III, at 1.10~1.40 m, the average TN removal rate was sharply promoted to 3.95 $g \cdot m^{-3} \cdot d^{-1}$ and 14.67 $mg \cdot L^{-1}$nitrate nitrogen was eliminated in this area. However, at 1.40~1.70 and 1.70~2.00 m, the removal rate was reduced to 1.78 and 0.94 g·m-3·d^{-1}, suggesting that the denitrification process was limited. Taking the COD variation in part III into consideration, the COD/TN ratio were respectively 2.85, 2.68, and 2.34 mg COD·$(mg\ TN)^{-1}$ at 1.10~1.40, 1.40~1.70 and 1.70~2.00 m, which were lower than the literature value (Pochana & Keller 1999). It is possible that some refractory organic matter was utilized during the denitrification process due to the lack of biodegradable organics. However, the standard COD determination method could not detect this refractory organic matter. It seemed that during the process of denitrification, the shortage of biodegradable organic matter restricted the elimination of TN.

After adding FA, the nitrogen variation trend was similar to before adding FA. However, the denitrification process was improved to a certain extent. 31.40 $mg \cdot L^{-1}$ of TN was eliminated in part three after the addition of FA, 6.39 $mg \cdot L^{-1}$ higher than before. Meanwhile, the COD removal rate was respectively 14.23, 7.10, and 3.73 $g \cdot m^{-3} \cdot d^{-1}$ at 1.10~1.40, 1.40~1.70, and 1.70~2.00 m, which were all higher than before. Also, 103.98 $mg.L^{-1}$ COD was degraded after adding FA, which was 37.43 $mg \cdot L^{-1}$ higher than before. We could conclude that adding FA could provide a high level of carbon

source for denitrification, resulting in the enhancement of TN elimination.

However, the variation of COD could demonstrate the changes in total organic matter. More details about the change rules in organic matter should be studied.

Fluorescence Spectrum Analysis

The current work elucidated and distinguished the transformation and alteration of organic matter in the SWIS. The analysis of 3DEEM integrated with PARAFAC was comprehensively utilized to quantify the variation of dissolved organic matter (DOM).

The spectra of 72 samples were applied to form the model components. Before PARAFAC modeling, FL solution 4.0 and DOM Flour toolbox were used to wipe off the influence of Raman and Rayleigh scattering. Moreover, all fluorescent data of samples were normalized by dividing by the TOC of each sample. 3-5 component models with non-negativity restrictions were performed. The loadings were converted to positive values and plotted. It was found that a 3-component model was sufficient to depict the dataset and minimize the residuals. Fig. 4 illustrates the position of maximum intensities of PARAFAC components.

The maximum intensity of C1 was located at Ex245/ Em410 (Fig. 4), which was associated with fulvic acid-like components (Region III) (Wünsch et al. 2019). The maximum intensities of C2 were located at Ex235/ Em275 and Ex235/ Em340, which were related or correlated to protein-like (such as tryptophan- and tyrosine-like) components (Regions I, II, and IV) (Arellano & Coble 2015, Ishii & Boyer 2012). The locations of maximum intensities of C3 were Ex270/ Em335 and Ex270/ Em460 due to the presence of humic acid-like organic matters (Region V) (Nebbioso & Piccolo 2012, Lyu et al. 2021).

As shown in Tables 3 & 4, there is no significant difference in the change of organic matter between with and without FA addition. At 0~1.10 m, organic matter (mainly protein-like substance, C2) was greatly consumed due to its aerobic degradation and nitrification process. Parts of them were utilized and adsorbed by microorganisms, while others were transformed into refractory substances (such as fulvic acid- and humic acid-like substances (C1, C3)), resulting in a decrease in biodegradability. The result was consistent with the variation of COD. However, at 1.10~1.40 m, the biodegradability increased because of the decrease of C1 and C3 and the increase of C2. It seemed that C1 and C3 were transformed into C2. As described above, the denitrification

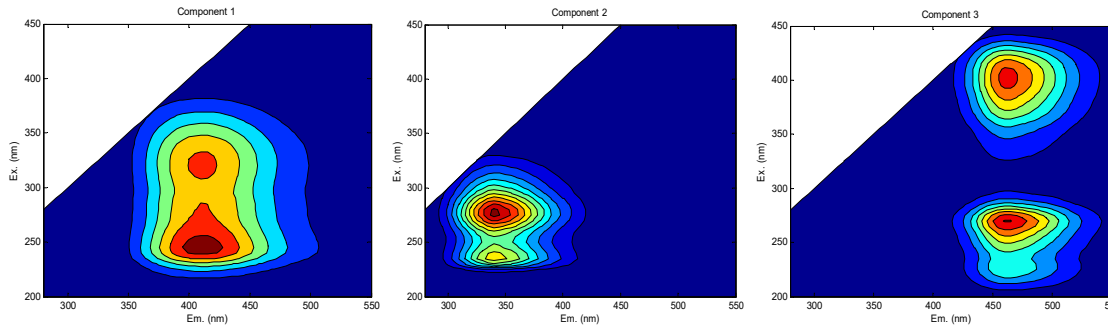

Fig. 4: Fluorescence spectra of three components distinguished by PARAFAC analysis. Component 1 (C1) location of maximum peak: Ex/Em=245/410, in Region III similar to peak fulvic acid-like (left); Component 2 (C2) location of maximum peak: Ex/Em=235,275/340, in Region I, II and IV similar to peak protein-like(middle); Component 3 (C3) location of maximum peak: Ex/Em=270/335,460, in Region V similar to peak humic acid-like (right).

Table 3: This was the biodegradability variation of organic matter before adding FA.

Dept [m]	C1 (fulvic acid-like)	C2 (protein-like)	C3 (humic acid-like)	Biodegradablity*
0	0.0201	0.9771	0.0028	0.0234
0.20	0.1603	0.7562	0.0835	0.3224
0.50	0.1903	0.6964	0.1133	0.4360
0.80	0.2314	0.6493	0.1193	0.5401
1.10	0.2399	0.6384	0.1217	0.5664
1.40	0.2312	0.6456	0.1232	0.5489
1.70	0.2476	0.6163	0.1361	0.6226
2.00	0.2538	0.6029	0.1433	0.6586

Table 4: This was the biodegradability variation of organic matter after adding FA.

Dept [m]	C1 (fulvic acid-like)	C2 (protein-like)	C3 (humic acid-like)	Biodegradablity*
0	0.1165	0.8790	0.0045	0.1377
0.20	0.1798	0.7338	0.0864	0.3628
0.50	0.2242	0.6769	0.0989	0.4773
0.80	0.2375	0.6425	0.1200	0.5564
1.10	0.2466	0.6235	0.1299	0.6038
1.40	0.2230	0.6565	0.1205	0.5232
1.70	0.2518	0.6121	0.1361	0.6337
2.00	0.2627	0.5948	0.1425	0.6812

*Biodegradablity = (C1+C3)/C2, which represents the biodegradability of organic matter. The smaller the biodegradability is, the easier the organic matter to be utilized by microorganisms.

process occurred at 1.10~2.00 m. Especially at 1.10~1.40 m, the denitrification rate was the highest. We could conclude that parts of refractory organic matter were degraded into biodegradable ones at 1.10~1.40 m, then implemented as carbon sources for denitrification. A similar result was reported by Nakhla and Farooq (2003). They demonstrated that the refractory organics were not able to be implemented as the carbon source for denitrification until the refractory organics were degraded into easily biodegradable organics. Moreover, after the addition of FA, 104.98 $mg \cdot L^{-1}$ of COD was degraded for the denitrification process, 57.75% higher than that before the addition of FA, which eliminated 31.40 $mg \cdot L^{-1}$ of TN, 28.64% higher than that before the addition of FA. It indicated that more FA-like matter was translated into protein-like matter after adding FA.

Overall, we could conclude that adding FA helped produce more easily degradable organic matter for denitrification, which enhanced the denitrification performance in the deep SWIS.

CONCLUSION

When a hydraulic loading was set as 8 $cm \cdot d^{-1}$ in DSWIS, the ammonia nitrogen, and COD could be efficiently removed before and after the FA addition. However, in the lower part, the removal efficiency of TN was insufficient due to the shortage of carbon sources which hindered the process of denitrification. Nevertheless, adding FA could facilitate the production of more easily degradable organics for denitrification, resulting in the enhancement of denitrification and the elimination of total nitrogen in the DSWIS.

ACKNOWLEDGEMENT

This work was sponsored by the Young Backbone Teachers Grant Scheme of Zhongyuan University of Technology, an Open Research Project on Heating and Air Conditioning Key Discipline in Higher Education Institutions in Henan Province(2017HAC108), Research Start-up Funds for High-level Talent Research of the Zhongyuan University of Technology, Natural Science Foundation of Henan (202300410512).

REFERENCES

Arellano, A.R. and Coble, P.G. 2015. Assessing carbon and nutrient inputs in a spring-fed estuary using fluorescence spectroscopy and discriminatory classification. Limnol. Oceanogr., 60 (3): 789-804.

Bieber, S., Snyder, S. A., Dagnino, S., Rauch-Williams, T. and Drewes, J.E. 2018. Management strategies for trace organic chemicals in water: A review of international approaches. Chemosphere, 195: 410-426.

Chen, F.M., Li, G.W., Li, X.G., Wang, H.Q., Wu, H.B., Li, J.X., Li, C.L., Li, W., Zhang, L.Y. and Xi, B.D. 2021. The cotreatment of old landfill leachate and domestic sewage in rural areas by deep subsurface wastewater infiltration system (SWIS): Performance and bacterial community. Environ. Pollut., 274(24): 115800.

Chen,W., Westerhoff, P., Leenheer, J.A. and Booksh, K. 2003. Fluorescence excitation–emission matrix regional integration to quantify spectra for dissolved organic matter. Environ. Sci. Technol., 37(24): 5701-5710.

Christianson, L.E., Lepine, C., Sibrell, P.L. and Penn, C. and Summerfelt, S.T. 2017. Denitrifying woodchip bioreactor and phosphorus filter pairing to minimize pollution swapping. Water Res., 121: 129-139.

E.P.A. (4th ed.) 2002. Standard methods for the examination of water and wastewater, China Environmental Science Press, pp.210.

Elliotts, S., Lead, J.R. and Baker, A. 2006. Characterisation of the fluorescence from freshwater, planktonic bacteria. Water Res., 40(10): 2075-2083.

Eregno, F.E. and Heistad, A. 2019. On-site treated wastewater disposal systems – The role of stratified filter media for reducing the risk of pollution. Environ. Int., 124: 302-311.

Gu, Y.F., Wei, Y., Xiang, Q.J., Zhao, K., Yu, X.M. Zhang, X.P., Li, C.N., Chen, Q., Xiao, H. and Zhang, X.H. 2019. C:N ratio shaped both the taxonomic and functional structure of microbial communities in livestock and poultry breeding wastewater treatment reactor. Sci. Total Environ. 651:625-633.

Ishii, S.K.L. and Boyer, T.H. 2012. Behavior of reoccurring PARAFAC components in fluorescent dissolved organic matter in natural and engineered systems: A critical review. Environ. Sci. Technol., 46(4): 2006-2017.

Jia, L.P., Cheng, X. L., Fang, L.C. and Huang, X. G. 2023.Nitrogen removal in improved subsurface wastewater infiltration system: Mechanism, microbial indicators and the limitation of phosphorus. J. Environ. Manage., 335: 117456.

Jia, L.P., Jiang, B.H., Huang, F. and Hu, X.M. 2019. Nitrogen removal mechanism and microbial community changes of bioaugmentation subsurface wastewater infiltration system. Bioresour. Technol., 294: 22-140.

Kawasaki, K. 2019. Paleomagnetism of the Mn wad deposit at Niimi hot springs, Hokkaido, Japan. Can. J. Earth Sci., 56(9): 973-982.

Li, W., Liang, C.L., Dong, L., Zhao, X. and Wu, H.M. 2021a.Accumulation and characteristics of fluorescent dissolved organic matter in loess soil-based subsurface wastewater infiltration system with aeration and biochar addition. Environ. Pollut., 269: 16100.

Li, Y.H., Peng, L.L., Zhang, Y., Li, H.B., Wang, Y.Y., Su, F. and Qian. J. 2023. Simultaneous removal of typical antibiotics and nitrogen by SWIS assisted by iron carbon micro-electrolysis. Chem. Eng. Res. Des.,192: 289-298.

Li, Y.H., Yang, L., Peng L.L., Liu, D.Z. and Li, H.B. 2021b. How does the operation time affect the performance and metabolomics of the subsurface wastewater infiltration bed? Desalin. Water Treat., 223: 146-153.

Lv, J.J., Dou, Y.Y., Gong, W.J., Duan, X.J., Hou, L.A., Zhang, L.Y., Xi, B.D. and Yu, S.L. 2019. Characterization of Dissolved Organic Matter in Hybrid Constructed Wetlands Using Three-Dimensional Excitation-Emission Matrix Fluorescence Spectroscopy. J. Water Chem. Techno., 41(2): 113-118.

Lv, J.J., Gong, W.J., Dou, Y.Y., Duan, X.J., Liu, H.F., Zhang, L.Y., Xi, B.D., Yu, S.L. and Hou, L.A. 2020. Spectroscopy and microbiological analysis of soil infiltration clogging in treating aged swine wastewater. Spectrosc. Spect. Anal., 40(5): 1541-1546.

Lyu, C., Liu, R., Li, X.J., Song, Y.H. and Gao, H.J. 2021. Degradation of dissolved organic matter in the effluent of municipal wastewater plant by a combined tidal and subsurface ^{flow} constructed wetland. J. Environ. Sci., 106: 171-181.

Markager, S., Stedmon, C.A. and Sondergaard, M. 2011. Seasonal dynamics and conservative mixing of dissolved organic matter in the temperate eutrophic estuary Horsens Fjord. Estuar. Coast. Shelf S., 92(3): 376-388.

Mazivila, S.J., Castro, R.A.E., Leitão, J.M.M. and da Silva, J.C.G.E. 2020. At-line monitoring of the salification process of the antiretroviral lamivudine-saccharinate salt using FT-MIR spectroscopy with multivariate curve resolution. Vib. Spectrosc., 106:102992.

Nakhla, G. and Farooq, S. 2003. Simultaneous nitrification-denitrification in slow sand filters. J. Hazard. Mater. 96(2-3): 291-303.

Nebbioso, A. and Piccolo, A. 2012. Molecular characterization of dissolved organic matter (DOM): a critical review. Anal. Bioanal. Chem. 405(1): 109-124.

Payne, E.G.I., Pham, T., Cook, P.L.M., Deletic, A., Hatt, B.E. and Fletcher, T.D. 2017. Inside story of gas processes within stormwater biofilters: Does greenhouse gas production tarnish the benefits of nitrogen removal? Environ. Sci. Technol., 51(7): 3703-3713.

Perujo, N., Sanchez-Vila, X., Proia, L. and Romaní, A.M. 2017. Interaction between Physical Heterogeneity and Microbial Processes in Subsurface Sediments: A Laboratory-Scale Column Experiment. Environ. Sci. Technol., 51(11): 6110-6119.

Pochana, K. and Keller, J. 1999. Study of factors affecting simultaneous nitrification and denitrification (SND). Water Sci. Technol., 39(6): 61-68.

Qin, S.N., Huang, F., Jiang, B.H. and Jia L.P. 2021.Evaluation of the removal performance in the long-term operation of bioaugmented subsurface wastewater infiltration systems under a high hydraulic loading rate. Environ. Technol. Inno.24: 101918.

Shokri, M., Kibler, K.M., Hagglund, C., Corrado, A., Wang, D.B., Beazley, M. and Wanielista. M. 2021. The hydraulic and nutrient removal performance of vegetated filter strips with engineered infiltration media for treatment of roadway runoff. J. Environ. Manag., 300: 113747.

Stevenson F. and Cole M. 1999. Cycles of soils: Carbon, nitrogen, phosphorus, sulfur, micronutrients, 2nd ed. John Wiley& Sons Inc., pp. 26.

Su, F., Li, Y.H., Qian, J., Wang, Y.Y. and Zhang, Y. 2023. Does the repeated freezing and thawing of the aerobic layer affect the anaerobic release of N_2O from SWIS? Sci. Total Environ., 859(2): 160313.

Urban-Rich, J., McCarty, J.T., Fernández, D., Acuña, J.L. 2006. Larvaceans and copepods excrete fluorescent dissolved organic matter (FDOM). J. Exp. Mar. Biol. Ecol., 332(1): 96-105.

Wünsch, U., Bro, R., Stedmon, C., Wenig, P. and Murphy, K. 2019. Emerging patterns in the global distribution of dissolved organic matter fluorescence. Anal. Methods, 11: 616 doi:10.1039/c8ay02422g.

Xu, J.J., Wu, X.H., Zhu, N.W., Shen, Y.W. and Yuan, H. P. 2020. Anammox process dosed with biochars for enhanced nitrogen removal: Role of surface functional groups. Sci. Total Environ., 748: 141367.

Yamaguchi, T., Moldrup, P., Rolston, D.E., Ito, S. and Teranishi, S. 1996. Nitrification in porous media during rapid, unsaturated water flow. Water Res., 30(3): 531-540.

Yang, L., Li, Y.H., Su, F. and Li, H.B. 2020. Metabolomics study of subsurface wastewater infiltration system under fluctuation of organic load. Curr. Microbiol., 77(2): 261-272.

Yang, P., Hou, R.R., Yuan, R.Y., Wang, F., Chen, Z.B., Zhou, B.H. and Chen, H.L. 2022. Effect of intermittent operation and shunt wastewater on pollutant removal and microbial community changes in subsurface wastewater infiltration system. Process Saf. Environ., 165: 255-265.

Yang, S.L., Zheng, Y.F., Mao, Y.X., Xu, L., Jin, Z., Zhao, M., Kong, H.N., Huang, X.F. and Zheng, X.Y. 2021.Domestic wastewater treatment for single household via novel subsurface wastewater infiltration systems (SWISs) with NiiMi process: Performance and microbial community. J. Clean. Prod., 279: 123434.

Ye, C., Hu, Z.B., Kong, H.N. Wang, X.Z. and He, S.B. 2008. A new soil infiltration technology for decentralized sewage treatment: Two-stage anaerobic tank and soil trench system. Pedosphere, 18(3): 401-408.

Yu, G.L., Peng, H.Y., Fu, Y.Q., Yan, X.J., Du, C.Y. and Chen, H. 2019. Enhanced nitrogen removal of low C/N wastewater in constructed wetlands with co-immobilizing solid carbon source and denitrifying bacteria. Bioresour. Technol., 280: 337-344.

Yuan, H.P., Nie, J.Y., Gu, L. and Zhu, N.W. 2016. Studies on affecting factors and mechanism of treating decentralized domestic sewage by a novel anti-clogging soil infiltration system. Environ. Technol., 37(23): 3071-3077.

Zhang, J., Song, F.H., Li, T.T., Xie, K.F., Yao, H.Y., Xing, B.S., Li, Z.Y. and Bai. Y.C. 2020. Simulated photo-degradation of dissolved organic matter in lakes revealed by three-dimensional excitation-emission matrix with regional integration and parallel factor analysis. J. Environ. Sci., 90(1): 310-320.

Zhang, L.Y., Ye, Y.B., Wang, L. Xi, B.D., Wang, H.Q. and Li, Y. 2015. Nitrogen removal processes in deep subsurface wastewater infiltration systems. Ecol. Eng., 77: 275-283.

Zheng, F.P., Tan, C.Q., Hou, W.Y., Huang, L.L., Pan J. and Qi S.Y. 2018a. Does the influent COD/N ratio affect nitrogen removal and N_2O emission in a novel biochar-sludge amended soil wastewater infiltration system (SWIS)? Water Sci. Technol., 78(2): 347-357.

Zheng, F.P., Zhao, Y., Li, Z.Q., Tan, C.Q., Pan, J., Fan, L.L., Xiao, L. and Hou, W.Y. 2018b. Nitrogen removal and N_2O emission by shunt distributing wastewater in aerated or non-aerated subsurface wastewater infiltration systems under different shunt ratios. Water Sci. Technol., 78(2): 329-338.